Asia Pacific Environmental and Occupational Health Journal (ISSN 2462 -2214), Vol 3 (2): 33 – 39, 2017

Synthesis of Titanium Oxide for The Application of Water Treatment

Joshua Zheyan Soo[1] and Sin Yew Keong [1]

[1]Faculty of Engineering, Multimedia University, Malaysia

Corresponding author: Sin Yew Keong; yksin@mmu.edu.my. Faculty of Engineering, Multimedia University, Persiaran Multimedia, 63100 Cyberjaya, Selangor, Malaysia.; +603-83125334

ABSTRACT

Introduction: Titanium dioxide (TiO_2) as a photocatalyst produces oxidizing radicals for water treatment. Treatment performance of TiO2 in natural light will be improved when doped with nitrogen. This is because the bandgap energy of TiO_2 will be lowered while its visible light absorbance will be increased.

Objective: To investigate the effects of nitrogen concentration on the photocatalytic behavior for TiO_2 particles synthesized via sol-gel method.

Method: TiO_2 and nitrogen-doped TiO_2 (N-TiO_2) powders were synthesized via sol-gel method. Calcination at 773 K followed by ball milling were done to obtain the TiO_2 powders. The effect of nitrogen concentration on the photocatalytic performance of TiO_2 was studied by varying the ratio of TTIP to urea. A filtration system was set up by incorporating TiO_2 powders with filter paper to obtain the optimum parameters for degrading methylene blue and treating bacteria-contaminated water. Characterizations of the synthesized powders include ultraviolet-visible (UV-vis) light spectroscopy, dynamic light scattering (DLS) measurement and scanning electron microscopy (SEM).

Result: Nitrogen doping in TiO_2 changes the appearance of powders from white to pale yellow. N-TiO_2 with TITP:urea of 1:2 has the lowest bandgap energy of 2.740 eV. However, TTIP:urea of 1:3 yields the highest visible light absorbance (VLA) and the smallest average particle size at 425 nm with the least polydispersity.

Conclusion: The optimum setup for removing methylene blue is by using N-TiO_2 with TTIP:urea ratio of 1:2 with 16 layers of filter paper which gives 98.42% methylene blue reduction. However, N-TiO_2 with TTIP:urea of 1:3 gives the optimum antibacterial performance with 65.26% less bacterial coverage.

Keywords: *Titanium dioxide, Photocatalysis, Water treatment, Methylene blue, Antibacterial treatment*

1. Introduction

The availability of clean freshwater is an important natural resource that ensures the survival of human civilisation. Although water covers 70% of the Earth's surface, only 2.5% of it is freshwater with only about 1% of it being accessible for human consumption (University of Michigan, 2006). The increase in human population and growth in industries and agriculture have caused the demand for clean freshwater to increase tremendously. At the same time, these factors have resulted in serious pollution of freshwater resources (Vaseashta, 2008).

Titanium dioxide (TiO_2) is a material that is classified in the group of transition metal oxides. It is usually considered as an n-type semiconductor as there is an oxygen deficiency in TiO_2 and the presence of bandgap energy in the material (Pelaez et. al., 2012). It commonly exists in the more photoactive anatase and the more stable rutile polymorphs (Pelaez et. al., 2012; Gupta & Tripathi, 2011). The bandgap differs for each type of crystal structure with purely anatase TiO_2 particles having an indirect bandgap of 3.2 eV while rutile phases have either a direct bandgap of about 3.0 eV or an indirect bandgap of about 3.1 eV (Gupta & Tripathi, 2011; Valencia et. al., 2010). The relationship between anatase and rutile phase TiO_2 are such that rutile can be derived

from anatase via anatase-to-rutile transformation (ART). ART is a reconstructive process which involves breaking and reforming of bonds usually in the presence of high calcination temperatures (Batzill et. al., 2006). During this process, the c-axis of the anatase polymorph experiences contraction which results in a reduction the overall volume by about 8% which increases the density of the polymorph and form rutile structures in the process (Hanaor & Sorrell, 2011).

The application of TiO_2 in water treatment is based on its role as a photocatalyst in the Advanced Oxidation Process (AOP). AOP is a process that produces powerful oxidizing radicals to decompose organic compounds into safer compound products such as carbon dioxide (CO_2) or water (Lee & Park, 2013). The antibacterial properties of TiO_2 utilizes the same AOP process to oxidize the target bacteria's cell membrane (Fagan et. al., 2015). This leads to the leakage of internal bacterial components including its cytoplasm and the death of the bacteria cell (Wang et. al., 2013). Being an indirect semiconductor, anatase TiO_2 has better photocatalytic behaviour than rutile polymorphs due to the longer electron-hole (e-h) pair life times which increases the chance of it participating in surface reactions (Ratan & Bansal, 2013). At the same time, the triangular arrangement of oxygen ions on the anatase crystal surface allow for more effective chemical absorption and reaction (Xu et. al., 2011).

However, due to its limited photocatalytic effectiveness in the ultraviolet (UV) light range, further modification to pure TiO_2 is suggested via nitrogen doping to form N-TiO_2. Nitrogen atoms are found to be easily incorporated in the pure TiO_2 structure due to its similar atomic size with oxygen that it intends to replace as well as having a small ionization energy with high stability (Sato et. al., 2005). The addition of nitrogen will correspond to a decrease in bandgap energy and greater visible light absorbance (VLA) by N-TiO_2 powders (Nolan et. al., 2012; Asahi et. al., 2001). Nolan et al. mentioned that this enhanced property is only present in anatase TiO_2 while a blue shift is observed for rutile polymorphs instead when nitrogen is added due to the lowering of the top of the TiO_2 valence band as well as lower energy of the 2p orbital levels of nitrogen when compared to the valence band of pure rutile (Nolan et. al., 2012). N-TiO_2 crystals displays a slower transformation from anatase to rutile which enhances its photocatalytic properties. At the same time, a reduction in mean diameter size is observed as nitrogen concentration increases (Larumbe et. al., 2015).

2. Materials and Method

The particles were based on the sol-gel method by Larumbe et al. (2015). All reagents that were used in this synthesis are of analytical grade and no further purification step is needed. TTIP was used as the titanium precursor while urea was used as the nitrogen precursor for N-TiO_2. In the first step, 5.7 ml of TTIP (Sigma-Aldrich, 97%) was mixed into 4.5 ml of ethanol solvent (QREC, 96%) using a magnetic stirring hot plate at room temperature. Motor speed setting 2 (approximately 430 rpm) was used throughout the stirring process. Next, drops of nitric acid (Sigma Aldrich, 70%) was added to the mixture until the pH level reaches 2 to prevent precipitation of the titanium alkoxide. The solution was then heated up to 50 °C and 1 ml of distilled water was added into the mixture to start the hydrolysis and gelation process. To produce the N-TiO_2 particles, two urea solutions were first prepared by dissolving 2.3126 g and 3.4234 g of urea crystals (Fisher Scientific, ≥99%) in distilled water to obtain the TTIP:urea molar ratio of 1:2 (2N-TiO_2) and 1:3 (3N-TiO_2) respectively. The prepared urea solutions were added into the alkoxide gel and then mechanically stirred. The gel was then dried at 70 °C for 2 hours before it is calcined at 500 °C for 1 hour. The calcined particles were then ball milled for 10 minutes to obtain the sample powders.

Before characterization was done, liquid suspension of the powders was prepared using ethanol dispersant at 0.01 g/mL concentration followed by sonication for 15 minutes. Characterization of the suspended powders was done using UV-vis spectroscopy to obtain the absorbance spectrum and the bandgap energy for all samples. Particle size and morphology of TiO_2 or N-TiO_2 thin films of all concentrations were studied using DLS measurment with a particle size analyser (Malvern Instruments) and SEM operating at 20 kV with 10000x magnification. The thin films were prepared through spin coating of the liquid suspension at 200rpm for 20 seconds followed by 1500rpm for another 20 seconds.

The photocatalytic ability of the synthesized TiO_2 and N-TiO_2 powders to degrade methylene blue

as well as to remove bacteria were tested in this work. A simple filtration system was set up using 16 layers of filter paper and 0.5 mL of the milled powders. For methylene blue degradation, 5 mL of methylene blue solution (concentration: 0.3 g/L) was fed into the system and the output sample was obtained. All setups was done at visible light condition except for TiO_2 where tests were done at visible light, dark and pure UV light conditions. A control was done using only filter papers to measure the effectiveness of the TiO_2 and N-TiO_2 powders. Characterization was done for the output solution using UV-vis spectroscopy and the peak absorbance at 661.86 nm was obtained. For antibacterial treatment, drain wastewater was fed into the same setup and the output water sample was swabbed on an agar plate. The condition of the agar plate, specifically the area of coverage of the agar plate was observed after 4 days. This was a cross-sectional study conducted among welders employed in small and medium sized establishments of automobile workshop in Malaysia.

3. Results

The synthesis of TiO_2 produces a powder with a mainly white appearance. Meanwhile, the 2N-TiO_2 and 3N-TiO_2 powders are found to be pale yellow in colour. On closer observation, traces of yellowish powder can be seen in the undoped TiO_2 samples. The UV-vis spectroscopy characterization of TiO_2, 2N-TiO_2 and 3N-TiO_2 yielded the following absorbance spectra as shown in Figure 1. From the absorbance spectra, the bandgap energy of the particles was estimated using Tauc plot of $(\alpha h\nu)^{1/2}$ vs hv through the absorption spectra. Extrapolation done on the Tauc plot provided an estimated bandgap value of 2.920, 2.740 and 2.780 eV for TiO_2, 2N-TiO_2 and 3N-TiO_2 respectively.

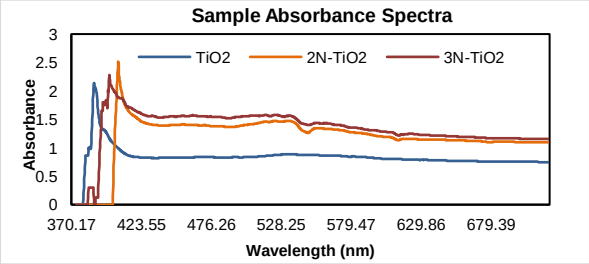

Figure 1. UV-vis absorption spectra of synthesized TiO_2 and N-TiO_2 powders.

The DLS measurement of the sample powder suspensions yielded the following results as tabulated in Table 1. The parameters measured are the cumulant mean size of the sample (Z-average) as well as the sample polydispersity (PDI). The images obtained from SEM at 10000x magnification are shown in Figure 2.

Table 1. Particle information obtained from DLS measurement.

Sample	Z-Average (nm)	PDI
TiO_2	506.0	0.457
2N-TiO_2	770.0	0.628
3N-TiO_2	425.0	0.390

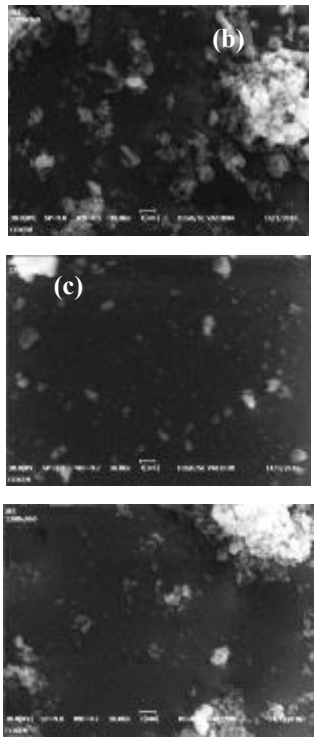

Figure 2. SEM images of (a) TiO_2 (b) 2N-TiO_2 and (c) 3N-TiO_2 thin films at magnification of 10000x.

From the SEM images, the histogram of particle size distribution was created for each sample as shown in Figure 3.

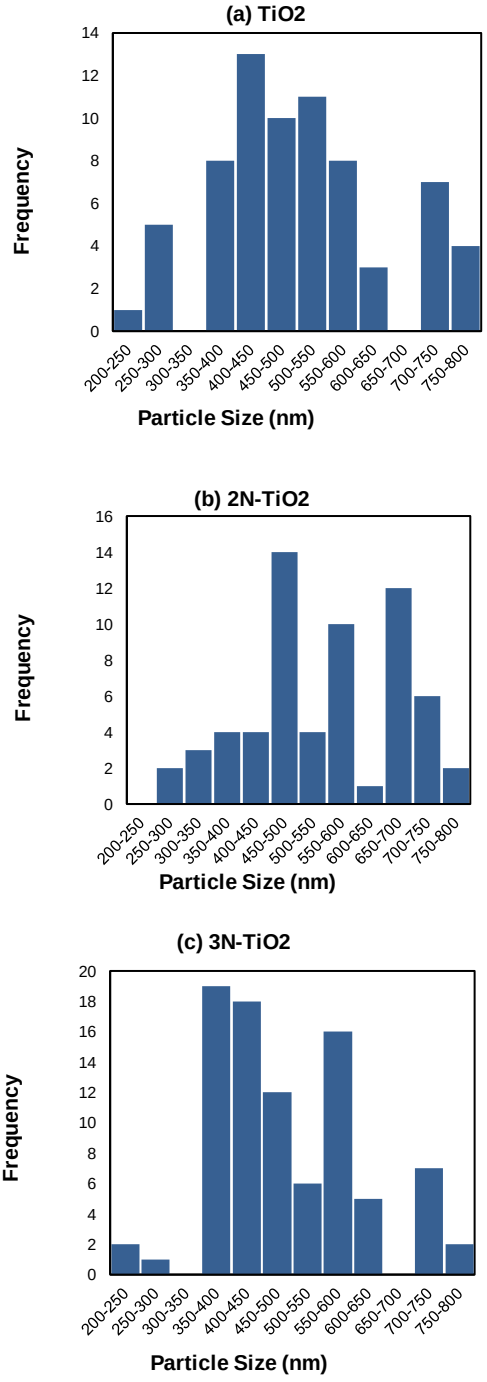

Figure 3. Histogram of particle size distribution of (a) TiO_2 (b) 2N-TiO_2 and (c) 3N-TiO_2 thin films.

In the water treatment test, the percentage of methylene blue reduction as well as the reduction in bacterial coverage for each setup was tabulated in Table 2.

Table 2. Percentage of methylene blue degradation for different setup.

Setup	Methylene Blue Reduction (%)	Bacterial Coverage Reduction (%)
Pre-treatment	0.00	0.00
Control	51.09	2.00
TiO_2	91.73	45.58
TiO_2 (UV)	86.87	7.23
TiO_2 (Dark)	73.86	2.00
2N-TiO_2	98.42	59.51
3N-TiO_2	97.85	65.26

4. Discussion

The change in the colour of N-TiO_2 (pale yellow) compared to undoped TiO_2 (white) showed that the addition of nitrogen dopant plays a role in altering the colour of the TiO2 particles (Nolan et. al., 2012; Li et. al., 2015). This observation can also be attributed to the change of band structure due to nitrogen addition which reduces the bandgap energy either through the addition of an N-level mid gap or the substitution of oxygen 2p orbitals with nitrogen 2p orbitals (Rane et. al., 2006; Mekprasat et. al., 2013). In accordance with the theory of photoluminescence, the lower bandgap energy of N-TiO_2 will result in an emission of photons of higher wavelength when an electron de-excites and falls from the conduction band to the valence band (Li, 2003). The traces of yellow powder in the undoped TiO_2 sample is deduced to be the result of unintended nitrogen doping with the origin to be from the nitric acid used during the synthesis process (Larumbe et. al., 2015).

The inference about the reduction of bandgap energy can be verified in the UV-vis absorbance spectra in Figure 1. The spectra showed that 2N-TiO_2 and 3N-TiO_2 have a red-shift in the spectra and higher VLA when compared to TiO_2. From the Tauc plot, the estimated bandgap value of TiO_2 of 2.920 eV is lower than the reported bandgap energy of pure TiO_2 in the literature review (Larumbe et. al., 2015). The traces of nitrogen doping from nitric acid may have contributed to the lower bandgap energy. Both bandgap energy values of 2N-TiO_2 and 3N-TiO_2 are significantly lower than that of TiO_2 which demonstrated the effect of nitrogen doping in reducing the bandgap energy of TiO_2. This also indicates that this

synthesis method has successfully inserted nitrogen atoms into the TiO_2 lattice structure (Nolan et. al., 2012). There is a slight 'blue-shift' observed in the peak absorbance wavelength from 2N-TiO_2 to 3N-TiO_2 in Figure 1 as well as an increase in bandgap energy value. This finding could probably be an effect of the presence of rutile in the doped TiO_2 where the addition of nitrogen in rutile polymorphs will result in an increase in bandgap energy (Nolan et. al., 2012). The additional nitrogen concentration in 3N-TiO_2 may have contributed to more interstitial replacement of oxygen molecules at the rutile polymorphs. However, the VLA level in the 3N-TiO_2 spectrum continues to show an increase across all visible light wavelengths shown in Figure 1. This finding is likely due to the decreasing particle size of TiO_2 as nitrogen concentration increases which allows for higher photon absorption (Egerton, 2014). However, the effect of the bandgap energy change is seen with a decrease in the gap between absorbance levels of 3N-TiO_2 and 2N-TiO_2 as the wavelength number increases. This can be related to a reduction in the number of lower energy photons that can be absorbed by 3N-TiO_2 due to the higher bandgap energy.

From the information obtained in Table 1, it can be seen that the Z-average particle diameter for all samples are within the range of hundreds of nm. In addition, all the samples with the exception of 2N-TiO_2 show a PDI reading of around 0.39 to 0.5 which indicates of a moderately broad particle size distribution. When comparing the Z-average for 3N-TiO_2 and TiO_2 particles, the characterization obtained a lower average particle diameter and PDI for the doped TiO_2. This verifies the inference made regarding the increase of VLA of 3N-TiO_2 seen in Figure 1 due to the smaller particle size in the sample powders. It can be inferred that the addition of nitrogen doping produces a higher ratio of anatase to rutile polymorphs in the 3N-TiO_2 sample. As the anatase polymorphs are smaller in dimension compared to rutile (Gupta & Tripathi, 2011), the higher anatase to rutile ratio produces a combination of lower average particle size as well as more monodispersed distribution. On the other hand, analysis of the results obtained for the 2N-TiO_2 showed an increase in Z-average and PDI value compared to the other two samples. Analysis of the SEM images in Figure 2 show that the single particle sizes are the main contributor to the larger Z-average value observed in Table 1. The larger particle sizes could also play a role in the lack of agglomeration observed in Figure 2(b) as the particles possess less surface energy compared to TiO_2 and 3N-TiO_2 particles (Cao, 2004).

From the results in Table 2, it can be seen the addition of TiO_2 powders inside the filtration setup assist in further reduction as seen in the reduced absorbance intensity of the output solution. However, the overall performance of TiO_2 is reduced when the treatment was done in dark conditions. This difference in performance showed strong evidence of TiO_2 being a photocatalyst when degrading methylene blue and deactivating bacteria cells. The addition of UV light provided a small improvement in overall treatment performance which is still substantially lower than the same setup in visible light. Although TiO_2 is considered a UV-light active material, the low power of the UV lamp used may not induce sufficient high energy photons for photocatalytic activity. The addition of nitrogen dopant significantly improves the performance of TiO_2 with both 2N-TiO_2 and 3N-TiO_2 setups show greater methylene blue and bacteria coverage reduction compared to TiO_2 at all conditions. This shows that the reduced bandgap energy and higher VLA of N-TiO_2 allow the absorbance of more photons for better photocatalytic performance. For 3N-TiO_2, the smaller particle size may have contributed to a better treatment performance. When comparing both doped TiO_2 particles, 2N-TiO_2 has a slight edge in performance than 3N-TiO_2 in degrading methylene blue. This higher performance is present in spite of the higher particle size of 2N-TiO_2 compared to other synthesized samples. This trend follows with that of the absorbance spectra and bandgap energy of the powders in Figure 1. This showed that optical properties play a more significant role than particle size in the photocatalytic performance of TiO_2 in organic chemical water treatment. As for the antibacterial test, Table 2 showed a lower percentage of bacteria coverage for 3N-TiO_2 treated water than that of 2N-TiO_2. This showed that particle size play a more important role than optical bandgap energy in photocatalytic antibacterial treatment of water sources.

5. Conclusion

In summary, TiO_2 and N-TiO_2 particles were synthesized using sol-gel method followed by

calcination at 500 °C and ball-milling to obtain its respective powders. Doping TiO_2 with nitrogen reduces its initial bandgap energy of 2.920 eV due to the interstitial replacement of oxygen molecules by nitrogen. 2N-TiO_2 which has TTIP:urea of 1:2 yields the lowest bandgap energy of 2.740 eV and the biggest 'red-shift' in absorbance relative to TiO_2. The increase in nitrogen concentration results in an increase in the VLA level of TiO_2. The morphology of TiO_2 particle changes with the variation of nitrogen concentration with the lowest average particle size and polydispersity was achieved using TTIP:urea of 1:3. A water treatment setup was made using layers of filter paper and TiO_2/N-TiO_2 powders. TiO_2 is shown to be able to degrade methylene blue through photocatalysis using AOP while N-TiO_2 powders exhibit overall higher photocatalytic performance than TiO_2. For organic chemical degradation; N-TiO_2 powders synthesized with TTIP:urea ratio of 1:2 provides the best result of 98.42% reduction. For antibacterial water treatment, N-TiO_2 powders synthesized with TTIP:urea ratio of 1:3 provide the best result with 65.26% reduction of bacteria coverage.

Acknowledgement

We would like to express our thanks to the Faculty of Engineering, MMU Cyberjaya for providing the necessary equipment and the laboratories needed to perform and complete this work.

References

Asahi, R., Morikawa, T., Ohwaki, T., Aoki, K., & Taga, Y. (2001). Visible-Light Photocatalysis in Nitrogen-Doped Titanium Oxides. Science, 293, 269-271.

Batzill, M., Morales, E., & Diebold, U. (2006). Influence of Nitrogen Doping on the Defect Formation and Surface Properties of TiO2 Rutile and Anatase. Physical Review Letters, 96(2).

Cao, G. (2004). Nanostructures & Nanomaterials: Synthesis, Properties & Applications. London: Imperial College Press.

Egerton, T. (2014). UV-Absorption—The Primary Process in Photocatalysis and Some Practical Consequences . Molecules, 19, 18192-18214.

Fagan, R., McCormack, D., Dionysiou, D., & Pillai, S. (2015). A review of solar and visible light active TiO_2 photocatalysis for treating bacteria, cyanotoxins and contaminants of emerging concern. Materials Science in Semiconductor Processing, 1-13.

Gupta, S., & Tripathi, M. (2011). A review of TiO_2 nanoparticles. Chinese Science Bulletin, 56, 1639-1657.

Hanaor, D., & Sorrell, C. (2011). Review of the anatase to rutile transformation. Journal of Material Science, 46, 855-874.

Larumbe, S., Monge, M., & Gomez-Polo, C. (2015). Comparative study of (N, Fe) doped TiO_2 photocatalysts. Applied Surface Science, 327, 490-497.

Lee , S.-Y., & Park, S.-J. (2013). TiO_2 photocatalyst for water treatment applications. Journal of Industrial and Engineering Chemistry, 19, 1761-1769.

Li, A. (2003). Excitation of Photoluminescence. (Jet Propulsion Laboratory, California) Retrieved January 16, 2016, from https://ned.ipac.caltech.edu/level5/Sept03/Li/Li4.html

Li, H., Hao, Y., Lu, H., Liang, L., Wang, Y., Qiu, J., . . . Yao, J. (2015). A systematic study on visible-light N-doped TiO_2 photocatalyst obtained from ethylenediamine by sol-gel method. Applied Surface Science, 344, 112-118.

Mekprasart, W., Khumtong, T., Rattanarak, J., Techidheera, W., & Pecharapa, W. (2013). Effect of Nitrogen Doping on Optical and Photocatalytic Properties of TiO_2 Thin Film Prepared by Spin Coating Process. Energy Procedia, 34, 746-750.

Nolan, N., Synnott, D., Seery, M., Hinder, S., Wassenhoven, A., & Pillai, S. (2012). Effect of N-doping on the photocatalytic activity of sol-gel TiO_2. Journal of Hazardous Materials, 211-212, 88-94.

Pelaez, M., Nolan, N., Pillai, S., Seery, M., Falaras, P., Kontos, A., . . . Dionysiou, D. (2012). A review on the visible light active titanium dioxide photocatalysts for environmental applications. Applied Catalysis B: Environmental, 125, 331-349.

Rane, K., Mhalsiker, R., Yin, S., Sato, T., Cho, K., Dunbar, E., & Biswas, P. (2006). Visible light-sensitive yellow $TiO_{2-x}N_x$ and Fe–N co-doped $Ti_{1-y}Fe_yO_{2-x}N_x$ anatase photocatalysts. Journal of Solid State Chemistry, 179(10), 3033-3044.

Ratan, J., & Bansal, A. (2013). Photocatalysis by Nanoparticles of Titanium Dioxide for Drinking Water Purification: A Conceptual and State-of-Art Review. Materials Science Forum, 764, 130-150.

Sato, S., Nakamura, R., & Abe, S. (2005). Visible-light sensitization of TiO_2 photocatalysts by wet-method N doping. Applied Catalysis A: General, 284(1-2), 131-137.

University of Michigan. (2006, April 1). Human Appropriation of the World's Fresh Water Supply.

(Global Change Courses) Retrieved November 19, 2015, from http://www.globalchange.umich.edu/globalchange2/current/lectures/freshwater_supply/freshwater.html

Valencia, S., Marin, J., & Restrepo, G. (2010). Study of the Bandgap of Synthesized Titanium Dioxide Nanoparticles Using the Sol-Gel Method and a Hydrothermal Treatment. The Open Materials Science Journal, 4, 9-14.

Vaseashta, A. (2008). Nanomaterials for Chemical-Biological-Physical Integrity of Potable Water. NATO Advanced Research Workshop on Water Treatment Technologies for the Removal of High-Toxicity Pollutants. Kosice.

Wang, J., Li, C., Zhuang, H., & Zhang, J. (2013). Photocatalytic degradation of methylene blue and inactivation of Gram-negative bacteria by TiO_2 nanoparticles in aqueous suspension. Food Control, 34, 372-377.

Xu, M., Wang, Y., Idriss, H., & Woll, C. (2011). Photocatalytic Activity of Bulk TiO_2 Anatase and Rutile Single Crystals Using Infrared Absorption Spectroscopy. Physical Review Letters, 106, 1-4.